TEAD4 regulates trophectoderm differentiation upstream of CDX2 in a GATA3-independent manner in the human preimplantation embryo

Stamatiadis, P.; Cosemans, G.; Boel, A.; Menten, B.; Sutter, P. de; Stoop, D.; ... ; Heindryckx, B.

Human Reproduction, Vol.37, No.8, pp. 1760–1773, 2022
Advance Access Publication on June 14, 2022 https://doi.org/10.1093/humrep/deac138

human reproduction

ORIGINAL ARTICLE *Embryology*

TEAD4 regulates trophectoderm differentiation upstream of CDX2 in a GATA3-independent manner in the human preimplantation embryo

P. Stamatiadis [1], G. Cosemans[1], A. Boel [1], B. Menten [2], P. De Sutter[1], D. Stoop[1], S.M. Chuva de Sousa Lopes[1,3], F. Lluis[4], P. Coucke[3], and B. Heindryckx [1]

[1]Ghent-Fertility And Stem cell Team (G-FaST), Department for Reproductive Medicine, Ghent University Hospital, 9000 Ghent, Belgium [2]Department of Biomolecular Medicine, Center for Medical Genetics, Ghent University Hospital, Ghent 9000, Belgium [3]Department of Anatomy and Embryology, Leiden University Medical Centre, Leiden 2333 ZA, The Netherlands [4]Department of Development and Regeneration, Stem Cell Institute, KU Leuven, Leuven 300, Belgium

*Correspondence address. Ghent-Fertility And Stem cell Team (G-FaST), Department for Reproductive Medicine, Ghent University Hospital, Corneel Heymanslaan 10, 9000 Ghent, Belgium. E-mail: bjorn.heindryckx@ugent.be https://orcid.org/0000-0003-0630-8420

Submitted on July 22, 2021; resubmitted on April 21, 2022; editorial decision on May 25, 2022

STUDY QUESTION: What is the role of transcriptional-enhanced associate (TEA) domain family member 4 (*TEAD4*) in trophectoderm (TE) differentiation during human embryo preimplantation development in comparison to mouse?

SUMMARY ANSWER: *TEAD4* regulates TE lineage differentiation in the human preimplantation embryo acting upstream of caudal-type homeobox protein 2 (*CDX2*), but in contrast to the mouse in a GATA-binding protein 3 (*GATA3*)-independent manner.

WHAT IS KNOWN ALREADY: *Tead4* is one of the earliest transcription factors expressed during mouse embryo preimplantation development and is required for the expression of TE-associated genes. Functional knock-out studies in mouse, inactivating *Tead4* by site-specific recombination, have shown that *Tead4*-targeted embryos have compromised development and expression of the TE-specific *Cdx2* and *Gata3* is downregulated. *Cdx2* and *Gata3* act in parallel pathways downstream of *Tead4* to induce successful TE differentiation. Downstream loss of *Cdx2* expression, compromises TE differentiation and subsequent blastocoel formation and leads to the ectopic expression of inner cell mass (ICM) genes, including POU Class 5 homeobox 1 (*Pou5f1*) and SRY-box transcription factor (*Sox2*). *Cdx2* is a more potent regulator of TE fate in mouse as loss of *Cdx2* expression induces more severe phenotypes compared with loss of *Gata3* expression. The role of *TEAD4* and its downstream effectors during human preimplantation embryo development has not been investigated yet.

STUDY DESIGN, SIZE, DURATION: The clustered regularly interspaced short palindromic repeats—clustered regularly interspaced short palindromic repeats (CRISPR)-associated genes (CRISPR-Cas9) system was first introduced in pronuclei (PN)-stage mouse zygotes aiming to identify a guide RNA (gRNA), yielding high editing efficiency and effective disruption of the *Tead4* locus. Three guides were tested (gRNA1-3), each time targeting a distinct region of Exon 2 of *Tead4*. The effects of targeting on developmental capacity were studied in *Tead4*-targeted embryos (n = 164—summarized data from gRNA1-3) and were compared with two control groups; sham-injected embryos (n = 26) and non-injected media-control embryos (n = 51). The editing efficiency was determined by next-generation sequencing (NGS). In total, n = 55 (summarized data from gRNA1-3) targeted mouse embryos were analysed by NGS. Immunofluorescence analysis to confirm successful targeting by gRNA1 was performed in *Tead4*-targeted embryos, and non-injected media-control embryos. The downregulation of secondary TE-associated markers Cdx2 and Gata3 was used as an indirect confirmation of successful *Tead4*-targeting (previously shown to be expressed downstream of *Tead4)*. Additional groups of gRNA1 *Tead4*-targeted (n = 45) and media control (n = 36) embryos were cultured for an extended period of 8.5 days, to further assess the developmental capacity of the *Tead4*-targeted group to develop beyond implantation stages. Following the mouse investigation, human metaphase-II (MII) oocytes obtained by IVM were microinjected with gRNA-Cas9 during ICSI (n = 74) to target *TEAD4* or used as media-control (n = 33). The editing efficiency was successfully assessed in n = 25 *TEAD4*-targeted human embryos. Finally, immunofluorescence analysis for TEAD4, CDX2, GATA3 and the ICM marker SOX2 was performed in *TEAD4*-targeted (n = 10) and non-injected media-control embryos (n = 29).

PARTICIPANTS/MATERIALS, SETTING, METHODS: A ribonucleoprotein complex consisting of a gRNA-Cas9 mixture, designed to target Exon 2 of *Tead4*/*TEAD4*, was microinjected in mouse PN stage zygotes or human IVM MII oocytes along with sperm. Generated embryos were cultured *in vitro* for 4 days in mouse or 6.5 days in human. In mouse, an additional group of *Tead4*-targeted and media-control embryos was cultured *in vitro* for an extended period of 8.5 days. Embryonic development and morphology were assessed daily, during culture *in vitro* of mouse and human embryos and was followed by a detailed scoring at late blastocyst stage. Targeting efficiency following gRNA-Cas9 introduction was assessed via immunostaining and NGS analysis.

MAIN RESULTS AND THE ROLE OF CHANCE: NGS analysis of the *Tead4*-targeted locus revealed very high editing efficiencies for all three guides, with 100% of the mouse embryos (55 out of 55) carrying genetic modifications resulting from CRISPR-Cas9 genome editing. More specifically, 65.22% (15 out 23) of the PN zygotes microinjected with gRNA1-Cas9, which exhibited the highest efficiency, carried exclusively mutated alleles. The developmental capacity of targeted embryos was significantly reduced (data from gRNA1), as 44.17% of the embryos arrested at the morula stage (2.5 days post coitum), coincident with the initiation of TE lineage differentiation, compared with 8.51% in control and 12.50% in sham control groups. High-quality blastocyst formation rates (Grade 3) were 8.97% in the gRNA1-targeted group, compared with 87.23% in the media-control and 87.50% in the sham group. Immunofluorescence analysis in targeted embryos confirmed downregulation of *Tead4*, *Cdx2*, and *Gata3* expression, which resulted from successful targeting of the *Tead4* locus. *Tead4*-targeted mouse embryos stained positive for the ICM markers Pou5f1 and Sox2, indicating that expression of ICM lineage markers is not affected. *Tead4*-targeted embryos were able to cavitate and form a blastocoel without being able to hatch. Extended embryo culture following zona pellucida removal, revealed that the targeted embryos can attach and form egg-cylinder-like structures in the absence of trophoblast giant cells. In human embryos, Exon 2 of *TEAD4* was successfully targeted by CRISPR-Cas9 ($n = 74$). In total, 25 embryos from various developmental stages were analysed by NGS and 96.00% (24 out of 25) of the embryos carried genetic modifications because of gRNA-Cas9 editing. In the subgroup of the 24 edited embryos, 17 (70.83%) carried only mutant alleles and 11 out of these 17 (64.70%) carried exclusively frameshift mutations. Six out of 11 embryos reached the blastocyst stage. In contrast to mice, human-targeted embryos formed blastocysts at a rate (25.00%) that did not differ significantly from the control group (23.81%). However, blastocyst morphology and TE quality were significantly compromised following *TEAD4*-targeting, showing grade C TE scores, with TE containing very few cells. Immunofluorescence analysis of *TEAD4*-targeted embryos ($n = 10$) confirmed successful editing by the complete absence of TEAD4 and its downstream TE marker CDX2, but the embryos generated retained expression of GATA3, which is in contrast to what we have observed and has previously been reported in mouse. In this regard, our results indicate that GATA3 acts in parallel with TEAD4/CDX2 towards TE differentiation in human.

LARGE SCALE DATA: N/A.

LIMITATIONS, REASONS FOR CAUTION: CRISPR-Cas9 germline genome editing, in some cases, induces mosaic genotypes. These genotypes are a result of inefficient and delayed editing, and complicate the phenotypic analysis and developmental assessment of the injected embryos. We cannot exclude the possibility that the observed differences between mouse and human are the result of variable effects triggered by the culture conditions, which were however similar for both mouse and human embryos in this study. Furthermore, this study utilized human oocytes obtained by IVM, which may not fully recapitulate the developmental behaviour of *in vivo* matured oocytes.

WIDER IMPLICATIONS OF THE FINDINGS: Elucidation of the evolutionary conservation of molecular mechanisms that regulate the differentiation and formation of the trophoblast lineage can give us fundamental insights into early implantation failure, which accounts for ~15% of human conceptions.

STUDY FUNDING/COMPETING INTEREST(S): The research was funded by the FWO-Vlaanderen (Flemish fund for scientific research, Grant no. G051516N), and Hercules funding (FWO.HMZ.2016.00.02.01) and Ghent University (BOF.BAS.2018.0018.01). G.C. is supported by FWO-Vlaanderen (Flemish fund for scientific research, Grant no. 11L8822N). A.B. is supported by FWO-Vlaanderen (Flemish fund for scientific research, Grant no. 1298722 N). We further thank Ferring Pharmaceuticals (Aalst, Belgium) for their unrestricted educational grant. The authors declare no competing interests.

TRIAL REGISTRATION NUMBER: N/A.

Key words: TEAD4 / TEA domain family member 4 / genome editing / CRISPR-Cas9 / mouse embryo / human embryo / preimplantation development / peri-implantation development

Introduction

The totipotent zygote holds the capacity to give rise to a multitude of different cell types through a series of highly regulated cell cycles and lineage decisions. The first lineage choice in mammalian preimplantation embryo development either leads to the formation of the pluripotent inner cell mass (ICM), which will give rise to the body of the embryo and the yolk sac, or formation of the multi-potent outer extra-embryonic trophectoderm (TE), which will give rise to the placenta. In mouse, initiation of the differentiation events occurs following three symmetrical divisions and compaction of the embryo at the eight-cell stage (Mihajlović and Bruce, 2017). During compaction, the blastomeres flatten and undergo increased cell-to-cell adhesion, while

the embryo adopts a more spherical, smoother shape. Concurrent with compaction each blastomere acquires apical-basolateral polarity and becomes polarized. Cell polarization is critical for cell fate specification as it leads to an asymmetric distribution of cellular components. At this stage, all the cells which inherit the apical domain will form the outer layer and further differentiate towards the TE lineage, while some cells begin to migrate to the inner part of the embryo, loose polarity and start to differentiate towards the ICM (Stephenson et al., 2012). Recent studies have identified the molecular pathways leading to the *de novo* establishment of the cell polarization in the mouse embryo. Zygotic expression of transcription factor AP-2 gamma (*Tfap2c*) and TEA domain transcription factor 4 (*Tead4*) followed by activation of Rash homologous (Rho) GTPase is necessary and sufficient for the establishment of cell polarization in the mouse embryo (Zhu et al., 2017, 2020).

The subsequent changes following compaction and polarization are supported by an underlying transcriptional network regulating differentiation to the distinct lineages. These transcriptions factors in mouse and human can be categorized into three groups based on their localization pattern. The first group (factors localized in the ICM), consists of SRY-box transcription factor 2 (*Sox2*), POU Class 5 Homeobox 1 (*Pou5f1*) and Nanog homeobox (*Nanog*), which regulate initiation and maintenance of pluripotency (Palmieri et al., 1994; Nichols et al., 1998; Mitsui et al., 2003; Chen et al., 2009; Keramari et al., 2010; Thomson et al., 2011; Bessonnard et al., 2014; Mulas et al., 2018; Heurtier et al., 2019). The second group (factors localized in the TE) contains factors regulating TE differentiation such as caudal-type homeobox 2 (*Cdx2*), GATA-binding protein 3 (*Gata3*) and *Tfap2c* (Auman et al., 2002; Werling and Schorle, 2002; Strumpf et al., 2005; Winger et al., 2006; Home et al., 2009; Choi et al., 2012). The third group contains transcription factors expressed both in the ICM and TE lineage, such as *Tead4*, which control lineage segregation (Yagi et al., 2007; Nishioka et al., 2008; Home et al., 2012; Knott and Paul, 2014; Paul and Knott, 2014; Miller and Hendrich, 2018).

Tead4 is part of the TEAD family of transcription factors and is identified to be one of the earliest transcription factors, expressed during embryonic genome activation (EGA), which is essential for TE-associated gene expression, TE differentiation and blastocoel formation. *Tead4* contains an evolutionary conserved 72 amino acid TEA DNA binding domain, which has a crucial function as *Tead4* coactivators bind the TEA domain, and regulate *Tead4* activity (Vassilev et al., 2001; Mahoney et al., 2005). Yagi et al. (2007) showed that *Tead4* expression is abundant in all cells of the developing embryo. Its mechanism of action remained unknown until Nishioka et al. (2009) identified signalling components that could interpret inside/outside blastomere positional information and spatially regulate *Tead4* activity.

Differences in polarity and cell adhesion between inner and outer cells lead to the differential activation of the Hippo pathway. The active/inactive state of the Hippo pathway controls the activity of large tumour suppressor (LATS) kinase, a downstream component of the Hippo pathway, which regulates the phosphorylation status of *Tead4* coactivators, Yes1-Associated Transcriptional Regulator (Yap1) and WW Domain Containing Transcription Regulator 1 (Wwtr1). The phosphorylation status of Yap1 and Wwtr1 is correlated with their ability to translocate in the nucleus, bind *Tead4* and activate the expression of TE lineage specifiers.

In more detail, in the apolar inner cells, the hippo pathway is active, and the *Tead4* transcriptional co-activators Yap1 and Wwtr1 are phosphorylated by LATS kinase. Phosphorylation leads to cytoplasmic retention and inhibits entry of Yap1 and Wwtr1 into the nucleus. As a result, both factors are retained and subsequently degraded in the cytoplasm, unable to partner with Tead4 and initiate the expression of TE lineage specifiers. In the polar outer cells, the Hippo pathway and LATS kinase are inactive, Yap1 and Wwtr1 are un-phosphorylated and can enter the nucleus and interact with Tead4, forming active Tead4-(Yap1-Wwtr1) complexes, which initiate transcription of TE-specific genes including *Cdx2* and *Gata3*. It is worth mentioning that although *Tead4* has a dominant role in TE differentiation; it is not the only factor involved. *Pou5f1* and *Cdx2* are co-expressed in the mouse preimplantation embryo, and exhibit mutual antagonism (reciprocal inhibition), leading to the eventual segregation and control of differentiation of their distinct lineages, the ICM and TE lineage, respectively (Niwa et al., 2005).

Mouse knock-out studies inactivating *Tead4* by site-specific recombination have shown that *Tead4*-targeted embryos have compromised development and *Cdx2/Gata3* expression is downregulated (Yagi et al., 2007; Nishioka et al., 2008; Ralston et al., 2010; Kaneko and DePamphilis, 2013; Rayon et al., 2014; Israel et al., 2019). The importance of the Hippo pathway in regulating Tead4 activity and subsequent TE differentiation was shown in studies where overexpression of the downstream component of the Hippo pathway—LATS kinase—led to phosphorylation and cytoplasmic retention of the Tead4 coactivators (Yap1-Wwtr1), thus preventing the formation of active Tead4-(Yap1-Wwtr1) complexes and subsequent expression of *Cdx2* and *Gata3* in the outer cells, compromising TE differentiation (Nishioka et al., 2009). Lorthongpanich et al. (2013) showed that in embryos lacking LATS kinase, Yap1–Wwtr1 are not phosphorylated in the inner cells, although the Hippo pathway is active. Unphosphorylated Yap1–Wwtr1 molecules enter the nucleus, form active complexes with Tead4 and initiate transcription of *Cdx2* in the inner cells. In this manner, Yap1 and Wwtr1 regulate *Tead4*-dependent transcription necessary for the expression TE lineage specifiers downstream of the Hippo signalling pathway.

Although the importance of *Tead4* in regulating TE differentiation in mouse has been well established by knock-out studies, the regulatory mechanism leading to TE differentiation in human embryos remains elusive. The role of *TEAD4* has only been investigated during the trophoblast transition of human embryonic stem cells (hESCs). Xiao et al. performed multiple gain- and loss- of function experiments and identified interspecies differences related to different transcription roles of *TEAD4*, *CDX2* and *GATA3* between mouse and hESCs. Clustered regularly interspaced short palindromic repeats (CRISPR)-Cas9 targeted downregulation of *TEAD4* in hESCs did not affect trophoblast transition, as *GATA3* expression remained unaffected. Furthermore, *CDX2*-targeted hESCs were still able to undergo trophoblast transition and overexpression of *CDX2* was insufficient to initiate trophoblast transition (Xiao et al., 2020). *GATA3* overexpression in hESCs led to spontaneous differentiation towards the TE lineage (Xiao et al., 2020). This is in stark contrast to what is occurring in mouse ESCs, where *Cdx2* overexpression has been shown to induce TE differentiation (Tolkunova et al., 2006). Overall, the aforementioned data point to distinct developmental programmes between mouse and human and a

more important role of *GATA3* towards the TE lineage formation in human embryos.

In this study, we investigated the role of *TEAD4* in TE differentiation during human embryo preimplantation development by performing a CRISPR-Cas9 mediated functional knock-out study and examined the effects of *TEAD4* locus disruption in human preimplantation development. Differences in the expression of ICM- and TE-specific markers, characteristic of their respective lineage, were examined. We further compared our human data with the mouse model, attempting to identify interspecies similarities/differences in the pathways orchestrating TE lineage segregation and differentiation.

Materials and methods

Ethical approval

Animal Ethics Committee of Ghent University Hospital approved the conducted mouse animal experiments under the ECD18-29. Ghent University Hospital Ethical Committee (EC UZG 2018/0908) and the Belgian Federal Commission for medical scientific research on human embryos (FCE-ADV_077_UZ Gent) approved the conducted experiments requiring the use of human gametes (sperm, oocytes) for gene editing. All donated human oocytes, sperm and embryos used in this study were obtained with signed informed consent. Donated human samples originated from 48 patient couples. For the mouse experiments 55 mice were killed.

Mouse superovulation for zygote collection

Female B6D2F1 mice aged from 6 to 12 weeks old, underwent ovarian stimulation by i.p. injection with 5 IU pregnant mare's serum gonadotrophin (PMSG; HOR-272, Boxmeer, The Netherlands) between 5:00 and 6:00 p.m. Forty-eight hours following PMSG injection, 5 IU hCG (CG10-1VL, Sigma-Aldrich, Belgium) were injected i.p. Injected female mice were allowed to mate overnight with a male mouse aged between 10 and 15 weeks in a male: female ratio of 1:1. Mated female mice were killed by cervical dislocation 18–19 h following hCG injection, and zygote cumulus complexes (ZCCs) were collected. The ZCCs were treated in 200 IU/ml hyaluronidase (H3506, Sigma-Aldrich, Belgium) at 37 °C for a maximum of 3 min to remove the cumulus cells. Then zygotes were subjected to four serial washes in drops of KSOM (MR-101, Sigma-Aldrich, Belgium) and finally were transferred to drops of KSOM supplemented with 0.4% bovine serum albumin (BSA; 12657, Millipore, France) in a triple gas incubator. KSOM dishes were covered with oil to avoid media desiccation. The zygotes were incubated for a minimum of 30 min prior to the initiation of the experiment.

Human oocyte collection

Immature germinal vesicle (GV) or metaphase I (MI) stage oocytes were donated from patients undergoing fertility treatment at the Department for Reproductive Medicine, Ghent University Hospital. Immature oocytes were subjected to conditions allowing IVM immediately following denudation and isolation from cumulus oocyte complexes. More specifically, GV stage oocytes were cultured for 24 h in Medicult® media (82214010, Cooper Surgical, The Netherlands) and MI oocytes were cultured for a maximum of 4 h in Cook Cleavage® media (37°C, 5% O_2, 6% CO_2) until polar body extrusion (G46302, Cook Ireland Ltd, Ireland). Identification of successful maturation was based on extrusion of the first polar body. Successfully matured metaphase II (MII)-arrested oocytes were transferred to fresh equilibrated Cook Cleavage® medium, until the experiment was conducted.

Human sperm preparation

Donated human sperm were frozen following collection, stored in liquid nitrogen and thawed at the day of the experiment. For the thawing process sperm, straws were removed from the liquid nitrogen and allowed to thaw at room temperature for a ± 10-min period. The straw was cut and the liquified sperm was released in a tube containing 1 ml of gamete buffer (GB; G46320, Cook Ireland Ltd, Ireland). The tube was centrifuged (300 g, 10 min), and following centrifugation the supernatant was discarded. Fresh GB was slowly added in the tube and sperm were allowed to swim up at 37°C for 1 h. Following the incubation period, the supernatant containing the high-quality motile sperm was collected and used for ICSI.

Mouse zygote microinjection

Intracytoplasmic injection of the mouse zygotes with the guide RNA (gRNA)-Cas9 ribonucleoprotein mixture (RNP) was performed using a piezo-driven injection system. The gRNA-Cas9 RNP mixture was aspirated in the needle until it reached a length equal to the diameter of the zygote and then was injected into the cytoplasm.

Human IVM oocyte microinjection

Initially, human sperm were immobilized in a drop containing polyvinylpyrrolidone (ART-4005-A, Cooper Surgical, The Netherlands). Then the sperm were aspirated and placed in a drop containing gRNA-Cas9 RNP mixture. An amount of RNP mixture equal to the diameter of the oocyte was aspirated along with the sperm and both were subsequently injected into the human IVM MII oocyte.

gRNA-Cas9 RNP preparation

Three CRISPR RNAs (crRNAs) were designed to target Exon 2 of *Tead4* by the *in silico* tool Chop Chop V3 and were manufactured by Integrated DNA technologies (IDT, Belgium; Labun *et al.*, 2019). The sequences are as follows: crRNA1 5′- GGAAGCTTCGCTCAATTTCG-3′—mm10 chr6:128270940-128270962, crRNA2 5′-CCGCAAAATTATCCTGACGG-3′—mm10 chr6:128270883–128270905, crRNA3 5′-ATAATTTTGCGGCGGCCGCA-3′ chr6: chr6:128270894–128270916. Each crRNA was resuspended in duplex buffer (1072547, IDT, Belgium) and mixed in a 1:1 molar ratio with *trans*-activating crRNA (tracrRNA; 1072532, IDT, Belgium). The mixture was subjected to conditions allowing crRNA-tracrRNA duplex formation (gRNA). First, the mixture was heated in a thermocycler to 95°C for 5 min and then allowed to cool at room temperature for 15 min, during which the duplex was formed. An equimolar amount of Cas9 protein (1072545, IDT, Belgium) was added. Optimem media (31985-62, Sigma-Aldrich, Belgium) was used to dilute the RNP complex to the final working concentration of 25 ng/µl. The human crRNA 5′-AAAATCATCCTGTCGGACGA-3′ hg38 chr12:2994959-2994981 was prepared in a similar manner.

Mouse/human embryo culture

Mouse zygotes were cultured in KSOM media supplemented with 0.4% BSA until the eight-cell stage (2.5 days post coitum (dpc)), and then transferred to Cook Blasto® (G46296, Cook Ireland Ltd, Ireland) media until 4.5 dpc. Similar to mouse, human microinjected oocytes were cultured in Cook Cleavage® (G46302, Cook Ireland Ltd, Ireland) until the eight-cell stage (3.0 days post-fertilization (dpf)) and then transferred to Cook Blasto®. Mouse and human embryos were cultured under the same conditions in a triple-gas incubator at 37°C with 5% O_2 and 6% CO_2.

Mouse/human blastocyst scoring/grading

Mouse blastocysts were scored according to the following criteria. Grade 1: small blastocyst with blastocoel equal to or less than half of the embryo volume. Grade 2: large blastocyst with blastocoel greater than half of the embryo volume or blastocyst with blastocoel cavity completely filling the embryo. Grade 3: expanded and hatching or completely hatched blastocyst (Cheng *et al.*, 2004). Human blastocysts were scored according to Gardner criteria (Schoolcraft *et al.*, 1999).

Mouse/human embryo DNA extraction and genotyping

DNA was extracted from single mouse and human embryos using Arcturus picopure™ DNA extraction kit (KIT0103, Life Technologies, Belgium) according to manufacturer instructions. Each embryo was transferred to a single PCR tube and a volume of 10 µl of proteinase K (15 µg/µl) was added. The PCR tubes from all the samples were collectively transferred to a thermocycler and were subjected to the following steps. First, the tubes were heated to 65°C for 4 h and then further heated to 95°C for 10 min to inactivate proteinase K. In the last step, the temperature was reduced to 4°C until the tubes were removed and stored in −20°C until further PCR analysis. Primer pair 1 (5′–3′) fw: GCACTGTGCACTCAGTTGAAG—rv: AACTGGCCT GTACTACTTGGG, mm10 chr6:128270752-128271193, size: 442 bp, and primer pair 2 fw: GAGTGCCTAGGTCATTGTGCT—rv: GGGA TGTTCTACCCCACCCA, hg38 chr12:2994516-2995261, size: 746 bp, were used for amplification of the targeted regions in mouse and human, respectively. KAPA2G Robust Hotstart readymix (Kapa Biosystems, Basel, Switzerland) containing KAPA2G Robust DNA polymerase was used for PCR amplification. Targeted genomic regions were amplified under the following PCR conditions: 5 min initial denaturation at 95°C, followed by 30 cycles of denaturation at 94°C for 1 min, annealing at 60°C for 1 min, extension at 72°C for 1 min and a final elongation at 72°C for 10 min. PCR amplicons were analysed in a fragment analyser (Advanced Analytical Technologies, Ankeny, IA, USA), and subsequent *in silico* analysis of fragment analyser data was performed using the software PROsize 3.0 according to the manufacturer (Advanced Analytical Technologies, Ankeny, IA, USA). Sufficiently amplified PCR products (>4 ng/µl) were subjected to next-generation sequencing (NGS; Illumina MiSeq) and the results were analysed by the bioinformatics tool Batch-GE (Boel *et al.*, 2016).

Immunocytochemistry and imaging

Embryos from the various developmental stages were fixed in 4% paraformaldehyde (P6148, Sigma, Belgium) for 20 min and then were washed three times in ice-cold PBS (AM9624, Fischer Scientific, Belgium). Then, the embryos were permeabilized in PBS containing 0.5% Triton-X (T8787, Sigma, Belgium;PBT 0.5%) for 20 min and further washed three times in a solution containing 0.1% Triton-X (PBT 0.1%). The embryos were subsequently transferred to blocking buffer consisting of PBT 0.1%, Triton X/10% foetal bovine serum (10270106, Life Technologies, Belgium) for 1 h at room temperature on an orbital shaker. Next, the embryos were incubated overnight at 4°C with primary antibodies according to the optimized concentrations, as described in Supplementary Table SI. The following day the embryos were washed three times in blocking buffer and then were incubated with secondary fluorescent antibodies for 1 h at room temperature, followed by extended washing in the washing/blocking solution. For the DNA staining, embryos were incubated for 30 min in 20 µg/ml Hoechst-33258. Finally, samples were imaged using a laser scanning confocal microscope (LSM900, Zeiss, Belgium). Figs 1–4 contain single confocal section images. The single confocal sections are focused on the plane containing the ICM and are representative of the embryo expression profile. Supplementary Fig. S1 contains maximum orthogonal projection images of ±25 sections.

Extended mouse embryo culture

Mouse blastocysts (4.5 dpc) were treated with acidic Tyrode's solution (A.T.; T1778, Sigma, Belgium) to remove the zona pellucida and then were transferred to eight-well, ibiTreat µ-plates (80826, Ibidi, Belgium) containing *in vitro* culture (IVC)1 media supplemented with ESC grade foetal calf serum (FB1001S, Biosera, Belgium). The medium was changed to IVC2 following successful attachment of embryos, which occurred after ∼2 days of *in vitro* culture. Embryo attachment was assessed by short rapid movement of the ibiTreat µ-plates. Attached embryos showed no sign of movement. The IVC1 and IVC2 media compositions were prepared as previously described (Bedzhov *et al.*, 2014).

Statistics

In silico statistical analysis was performed using Graphpad Prism ver. 9.0.1, (Graphpad Software Inc, USA). A chi-squared test was performed (significance level of *P*-value was 0.05) to compare the developmental competency among different groups. Differences in the total cell number, $Sox2^+$ and $Cdx2^+$ cells between *Tead4*-targeted and the media-control group were analysed by a two-tailed unpaired Student's t-test. Differences were considered significant at $P < 0.0001$.

Results

Mouse Tead4-targeted embryos exhibit impaired development and compromised TE lineage differentiation

In order to target *Tead4*, three crRNAs (crRNA1-3) were *in silico* designed to target Exon 2 of *Tead4*, aiming to identify the gRNA-Cas9 yielding the highest efficiency (Fig. 1a). The designed gRNA-Cas9 complexes were microinjected in pronuclei (PN) stage zygotes (n = 164). Two additional control groups were included: a sham-injected group (n = 26) and a media-control group (n = 51). NGS analysis in 4.5 dpc

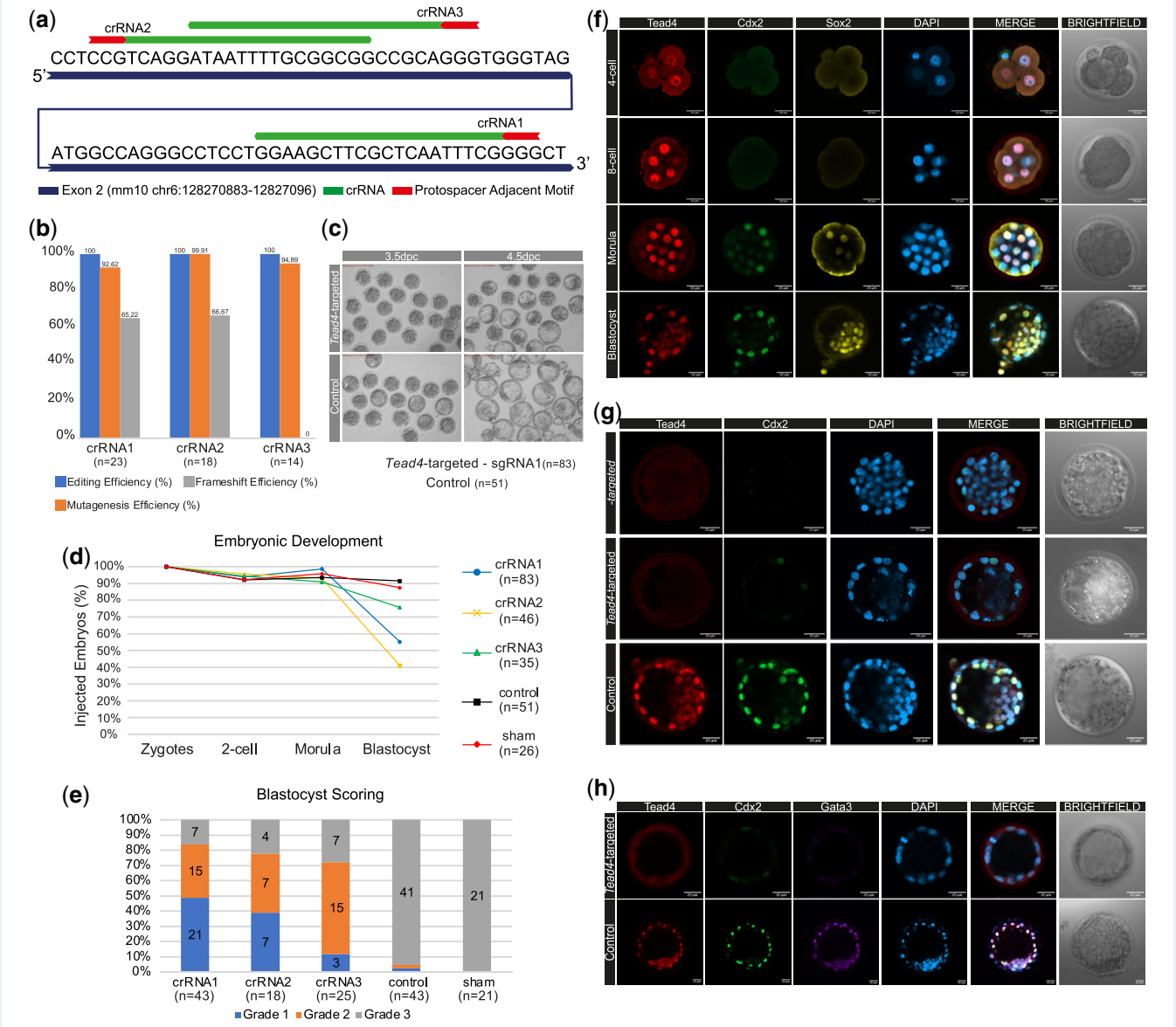

Figure 1. Targeting *Tead4* in mouse preimplantation embryos. (**a**) Schematic representation of the targeted Exon 2 (mm10 chr6:128270883–12827096) of the *Tead4* and the nucleotide sequences of the custom-designed crRNAs complementary to the targeted TEA domain. (**b**) Comparison of editing, mutagenesis, and frameshift efficiencies between the guides crRNA1, crRNA2 and crRNA3. The percentages are based on the number and identity of reads generated following NGS of single 4.5 dpc mouse embryos. (**c**) Representative phenotypic outcomes following BF imaging embryos microinjected with gRNA1-Cas9 (n = 83) and media-control embryos (n = 51) following 3 and 4 days of culture. (**d**) Detailed embryonic development kinetics based on morphological criteria of *in vitro*-cultured crRNA1 (n = 83), crRNA2 (n = 46) or crRNA3 (n = 35) microinjected embryos, with their respective media-control (n = 51) and sham (n = 26) injected control groups. Developmental rates of crRNA1 and crRNA2 microinjected embryos differed significantly from the control group (chi-squared test, $P = 0.0343$) in contrast to the crRNA3 group (chi-squared test, $P = 0.2932$). (**e**) Blastocyst scoring of *Tead4*-targeted (crRNA1-3), media-control and sham embryos. Evaluation of the blastocyst morphology was performed according to the following criteria Grade1: Small blastocyst with blastocoel equal to or less than half of the embryo volume. Grade2: Large blastocyst with blastocoel greater than half of the embryo volume or blastocyst with a blastocoel cavity completely filling the embryo Grade3: expanded and hatching or completely hatched blastocyst. (**f**) Immunofluorescence analysis of control embryos following *in vitro* culture for Tead4 (red), Cdx2 (green), Sox2 (yellow) and DAPI (blue) in four distinct developmental stages (four-, eight-cell, morula and blastocyst). (**g**) Immunofluorescence analysis of *Tead4*-targeted and media-control embryos for Tead4 (red), Cdx2 (green) and DAPI (blue) following 4 days of *in vitro* culture. (e) Immunofluorescence analysis of *Tead4*-targeted and control embryos for Tead4 (red), Cdx2 (green), Gata3 (purple) and DAPI (blue) following 4 days of *in vitro* culture. *Gata3* expression was completely abolished in *Tead4*-targeted embryos. TEA, transcriptional-enhanced associate; Tead4, TEA domain family member 4; CRISPR, clustered regularly interspaced short palindromic repeats; crRNAs, CRISPR RNAs; NGS, next generation sequencing; dpc, days post coitum; BF, bright field; gRNA1, guide RNA1; Cdx2, caudal-type homeobox protein 2; Sox2, SRY-box transcription factor; Gata3, GATA-binding protein 3; DAPI, 4',6'-diamidino-2-phenylindole.

embryos allowed comparison of the crRNAs in terms of editing efficiency (% embryos with introduced mutations), mutagenesis efficiency (% edited alleles per embryo) and frameshift efficiency (% embryos carrying exclusively frameshift mutations; Fig. 1b). In the crRNA1 group (n = 23) the editing efficiency was 100%, the mutagenesis efficiency was 92.62% and the frameshift efficiency was 65.22% (Fig. 1b and Supplementary Table SII). In the crRNA2 group (n = 18), the editing efficiency was 100%, the mutagenesis efficiency was 99.91% and the frameshift efficiency was 66.67% (Fig. 1b and Supplementary Table SIII). In the crRNA3 group (n = 14), the editing efficiency was 100%, the mutagenesis efficiency was 94.89% and the frameshift efficiency was 0% (Fig. 1b and Supplementary Table SIV). The crRNA1 was selected for further mouse experiments owing to the larger size of induced editing events, which are expected to have a higher impact on *Tead4* locus (Supplementary Table SII).

The developmental effects following *Tead4*-targeting started from the morula stage coincident with the timing of initiation of TE differentiation. Following gRNA1-Cas9 introduction, approximately half −44.87% (n = 35) of the targeted embryos arrested at the morula stage without forming any blastocoel (Fig. 1c–e and Supplementary Table SV) compared with 8.51% (n = 4) in media-control and 12.50% (n = 3) in sham-control groups. Grade 3 blastocyst rates were 8.97% (n = 7) in the targeted group, compared with 87.23% (n = 41) in the media-control and 87.50% (n = 21) in the sham group (Fig. 1e). Although hatching was initiated, *Tead4*-targeted embryos were not able to fully hatch independently. Developmental rates of gRNA1-Cas9 and gRNA2-Cas9 microinjected embryos differed significantly from the control group (chi-squared test, $P = 0.0343$) in contrast to the gRNA3-Cas9 group (chi-squared test, $P = 0.2932$).

Immunofluorescence analysis in Tead4-targeted mouse embryos revealed downregulation of TE-specific markers Cdx2 and Gata3

Initially, immunofluorescence staining was applied in control embryos from four developmental stages: four-cell (n = 8), eight-cell (n = 10), morula (n = 13) and blastocyst stage (n = 17) in order to establish a timeline of *Tead4* expression and protein localization during preimplantation development. Tead4 signal was identified in the nucleus of four-cell embryos and the nuclei of all blastomeres in the eight-cell and morula stage embryos (Fig. 1f). *Tead4* expression preceded *Cdx2* expression in control embryos, with the latter being initiated at the 16-cell stage (Fig. 1f). Sox2 expression was first identified in the inner cells of the developing morula (Fig. 1f). In late blastocysts, Tead4 was identified in both the blastomeres of the TE and ICM lineage, with the latter showing a lower signal (Fig. 1f).

Next, immunofluorescence analysis was used to validate the editing results, assess Tead4 protein expression, and its downstream effects. For the purpose of immunostaining, an additional group was microinjected with gRNA1-Cas9 (n = 58; Supplementary Table SV). Embryos from various developmental stages were stained for Tead4/Cdx2/Gata3 (n = 24 out of 58). In all embryos stained, *Tead4* and *Cdx2* expression was downregulated (Fig. 1g, e, 2a and Supplementary Fig. S1). Targeted embryos, which formed Grade 3 blastocysts (n = 7), retained expression of *Cdx2* in two to three cells per confocal section, while *Tead4* expression was completely downregulated (Figs. 1g and e and 2a and Supplementary Fig. S1). The arrested morula stage embryos were identified by absence of *Cdx2* expression (Fig. 1g). Gata3 was not detected in any of the immunostained embryos, including the embryos which formed Grade 3 blastocysts (Fig. 1e).

In order to provide a more extensive characterization and exclude the possibility of residual Tead4 protein expression in *Tead4*-targeted embryos, immunofluorescence analysis was performed and multiple confocal sections per embryo were taken (±25 sections) aiming to provide maximum orthogonal projection images (Supplementary Fig. S1a). Next, as a confirmation, DNA from the imaged embryo was extracted immediately after immunofluorescence analysis, and was subjected to NGS, to be able to link the phenotypic outcome to a specific genotype. Embryos successfully edited carrying frameshift only mutations, showed complete absence of Tead4 protein (*Tead4*-targeted embryos 1–3; Supplementary Fig. S1a). Mosaic embryos, partially edited—57.88% mutagenesis efficiency (*Tead4*-targeted embryos 4; Supplementary Fig. S1a) retained *Tead4* expression. Detailed comparison of the total cell number, $Sox2^+$ cells and $Cdx2^+$ cells following differential staining of the z-stacked embryo images, revealed that the total cell number and the $Cdx2^+$ cell number was significantly lower in the *Tead4*-targeted group, whereas the mean number of $Sox2^+$ cell number did not differ significantly between the two groups (Supplementary Fig. S1b–d).

Expression of ICM markers Sox2 and Pou5f1 remains unaffected in Tead4-targeted mouse embryos

To further examine if the ICM lineage is affected, we immunostained for the ICM lineage specifier *Sox2* in two distinct developmental stages (eight-cell and blastocyst stage; n = 23 out of 58; Fig. 2a). In our experiments, *Sox2* expression in *Tead4*-targeted embryos remained unaffected, similar to the control group, and we did not identify premature expression of *Sox2* in eight-cell *Tead4*-targeted embryos (Fig. 2a and Supplementary Fig. S1c). Immunostaining of *Tead4*-targeted 4.5 dpc embryos revealed that all cells stained positive for the pluripotency factor Pou5f1 (n = 11 out of 58; Fig. 2b).

To further assess the developmental potential of *Tead4*-targeted blastocysts, an additional group was microinjected with gRNA1-Cas9 (n = 45), and targeted embryos were plated *in vitro* in parallel to control embryos (n = 36) under conditions supporting peri- and post-implantation development (Supplementary Table SVI). Successful editing of *Tead4*-targeted embryos was indirectly judged based on the developmental rates of the embryos selected for plating; 46.51% arrested at morula stage, 9.3% formed Grade 3 blastocysts (Supplementary Table SVI), which matched the developmental rates of the NGS confirmed edited embryos, 43.48% arrested at morula stage and 8.70% formed Grade 3 blastocysts (Supplementary Table SV). Following zona pellucida removal by A.T. treatment, three *Tead4*-targeted embryos were able to attach and form egg-cylinder-like structures, which lacked the surrounding presence of trophoblast giant cells (Fig. 2c and Supplementary Table SVI). However, resulting outgrowths were not analysed by NGS to determine mutagenesis efficiency and identification of their genotype.

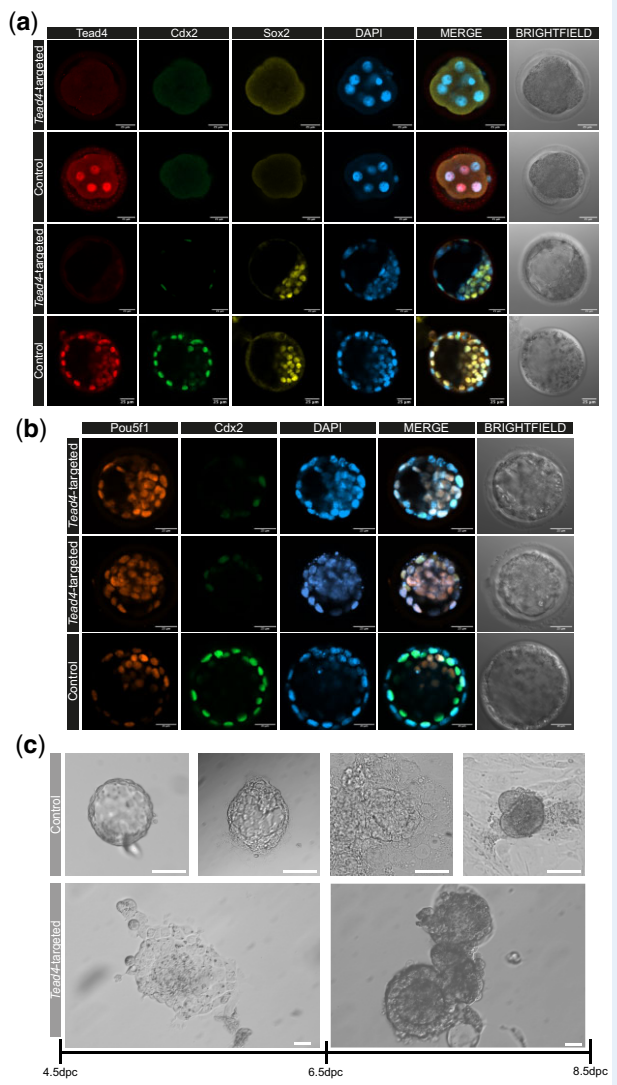

Figure 2. Molecular characterization of the ICM in mouse preimplantation embryos. (**a**) Immunofluorescence analysis of *Tead4*-targeted and media-control mouse embryos for Tead4 (red), Cdx2 (green), Sox2 (yellow) and DAPI (blue) in two distinct developmental stages (eight-cell and blastocyst stage). (**b**) Immunofluorescence analysis of *Tead4*-targeted and control embryos for Pou5f1 (orange), Cdx2 (green) and DAPI (blue). (**c**) Application of the post-implantation model in *Tead4*-targeted and control mouse embryos (Scale bar: 25μm). ICM, inner cell mass; Tead4, TEA domain family member 4; Cdx2, caudal-type homeobox protein 2; Sox2, SRY-box transcription factor; Pou5f1, POU Class 5 homeobox 1; DAPI, 4',6'-diamidino-2-phenylindole.

TEAD4, SOX2 and CDX2 expression pattern in human preimplantation embryos

To establish a timeline of *TEAD4* expression during human preimplantation development, immunofluorescence analysis was first applied in media-control embryos (n = 29; non-targeted) from various developmental stages (8-, 16-cell and blastocyst), which were surplus after fertility treatment at Ghent University Hospital, Ghent, Belgium. A subset of embryos (24 out of 29) was stained against TEAD4/CDX2/SOX2. TEAD4 was detected in the cytoplasm of 8-cell embryos (n = 6), while at the 16-cell morula stage (n = 7) and the blastocysts (n = 11), TEAD4 was detected in the nucleus of all cells (Fig. 3a). *SOX2* expression was detected from the 8-cell stage, and it was abundant in all cells of the 16-cell morula. All the nuclei until early blastocyst stage embryos stained positive for SOX2 (Fig. 3a). In the late blastocyst stage, SOX2 was restricted to the ICM and in a small number of TE cells (Fig. 3a). CDX2 was absent until the morula stage (32-cell) and was first detected following blastocoel formation in the TE lineage and remained abundant in all cells of the TE in blastocyst stage embryos (Fig. 3a). The remaining 5 embryos (5 out of 29) were cultured until blastocyst stage and were stained for GATA3, along with TEAD4/CDX2. GATA3 was expressed in all the TE cells of the human blastocysts (Fig. 4b).

TEAD4 targeting in human preimplantation embryos

Similar to what we previously described in mouse, to target *TEAD4* we designed a crRNA targeting Exon 2. This crRNA exhibited high *in silico* predicted on-target editing efficiency and no predicted off-target sites, taking mismatches of maximal two base pairs into account (Fig. 3b). In the targeted group, the gRNA-Cas9 mixture was microinjected concurrent with sperm during ICSI in MII oocytes obtained by IVM (n = 74). The media-control group was injected only with sperm (n = 33). Embryos were cultured until 6.5 dpf. A subset of targeted embryos (n = 25) was subjected to NGS and 24 embryos were identified to be successfully edited, resulting in an editing efficiency of (96.00%). From the 24 edited embryos, 17 (70.83%) embryos carried only mutant alleles and 11 out of 17 (64.70%) carried frameshift mutations (Supplementary Table SVII) exclusively. From the embryos that reached the blastocyst stage, six carried frameshift mutations exclusively. Representative targeted blastocysts, including their morphology and mutational signature, are presented in Fig. 3c.

The developmental capacity of the *TEAD4*-targeted embryos did not differ significantly compared with the control group ($P = 0.1479$). Following EGA, which occurs at the four- to eight-cell stage, 34.62% of targeted embryos reached the eight-cell stage compared with 33.33% of the control group. The blastocyst development rate of targeted embryos was 25.00% compared with 23.81% of the control group (Fig. 3d and Supplementary Table SVIII). However, the blastocyst morphology and quality of the targeted group were compromised as the resulting blastocysts were characterized by a Grade C TE score, with TE containing very few cells. Detailed development rates are described (Fig. 3d and Supplementary Table SVIII).

Immunofluorescence analysis in the targeted blastocysts confirmed successful interruption of the *TEAD4* locus (n = 10). Targeted embryos were also immunostained for the TE marker CDX2. Interruption of the *TEAD4* locus resulted in downregulation of *CDX2* in all cells of the developing embryo (Fig. 3e). We further immunostained for the ICM marker SOX2, indicative of the pluripotent state of the ICM lineage. The *SOX2* expression pattern remained similar in *TEAD4*-targeted and media-control embryos. (Fig. 4a). In the final stage of our investigation, we immunostained for the TE marker GATA3. Interestingly, *GATA3* expression remained unaffected in *TEAD4*-targeted embryos (Fig. 4b).

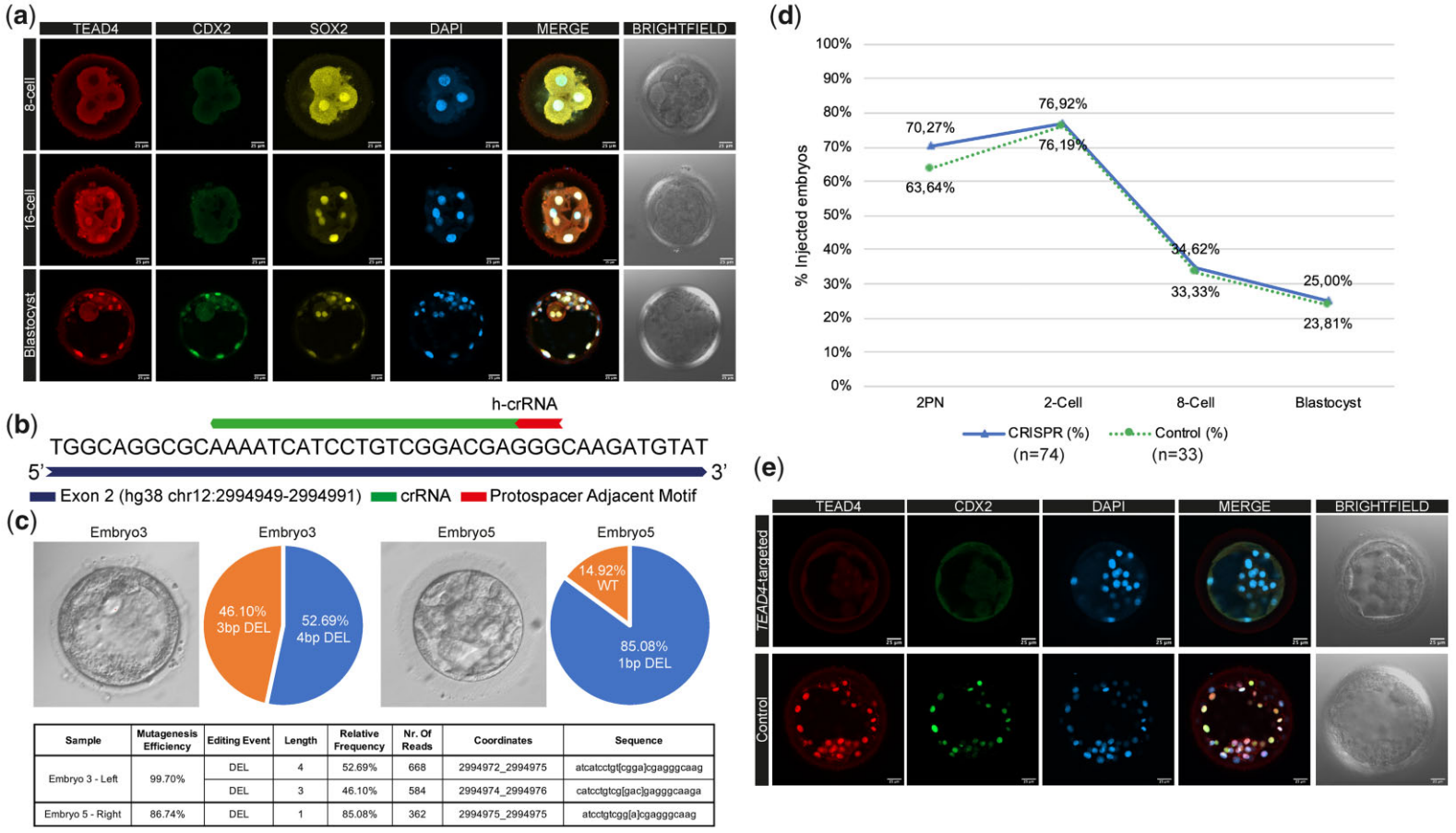

Sample	Mutagenesis Efficiency	Editing Event	Length	Relative Frequency	Nr. Of Reads	Coordinates	Sequence
Embryo 3 - Left	99.70%	DEL	4	52.69%	668	2994972_2994975	atcatcctgt[cgga]cgagggcaag
		DEL	3	46.10%	584	2994974_2994976	catcctgtcg[gac]gagggcaaga
Embryo 5 - Right	86.74%	DEL	1	85.08%	362	2994975_2994975	atcctgtcgg[a]cgagggcaag

Figure 3. Targeting *TEAD4* in human preimplantation embryos. (**a**) Immunofluorescence analysis of control embryos following *in vitro* culture for TEAD4 (red), CDX2 (green), SOX2 (yellow) and DAPI (blue) in three distinct developmental stages (8-, 16-cell and blastocyst). (**b**) Schematic representation of the targeted Exon 2 (hg38 chr12:2994949–2994991) of *TEAD4* and the nucleotide sequences of the custom-designed crRNA. (**c**) Representative phenotypes of targeted blastocysts along with detailed genomic analysis following NGS, including the mutagenesis efficiency, mutational spectrum, type and frequency of each editing event. (**d**) Developmental rates of *TEAD4*-targeted (n = 74) and control (n = 33) embryos. Chi-squared test ($P = 0.1479$) revealed no significant difference between the two groups. (**e**) Immunofluorescence analysis of *TEAD4*-targeted and control embryos for TEAD4 (red), CDX2 (green) and DAPI (blue). The exact editing efficiency and mutational signature of the displayed blastocyst can be found in Supplementary Table SVI—Embryo 17. PN, pronuclei; DEL, deletion; Tead4, TEA domain family member 4; Cdx2, caudal-type homeobox protein 2; SOX2, SRY-box transcription factor; crRNA, CRISPR RNA; NGS, next generation sequencing; DAPI, 4',6'-diamidino-2-phenylindole.

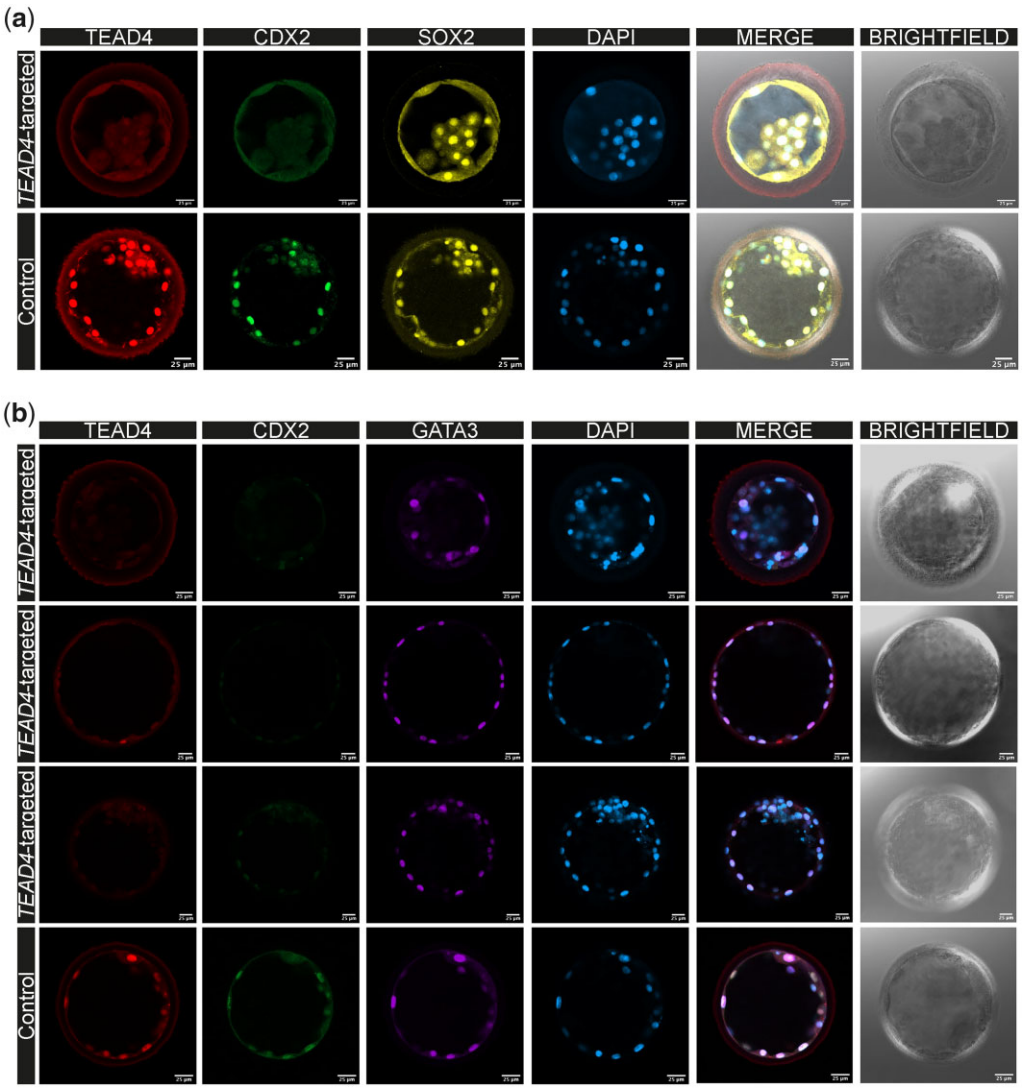

Figure 4. Molecular characterization of human targeted and control embryos. (**a**) Immunofluorescence analysis of *TEAD4*-targeted and control embryos for TEAD4 (red), CDX2 (green), SOX2 (yellow) and DAPI (blue). (**b**) Immunofluorescence analysis of *TEAD4*-targeted and control embryos for TEAD4 (red), CDX2 (green), GATA3 (purple) and DAPI (blue). DNA was extracted from the immunostained blastocysts and was subjected to NGS. The exact editing efficiencies and mutational signatures can be found in Supplementary Table SVII—embryos 23, 24 and 25 as they are presented from top to bottom in Fig. 4b. TEAD4,transcriptional-enhanced associate domain family member 4; CDX2, caudal-type homeobox protein 2; SOX2, SRY-box transcription factor; GATA3, GATA-binding protein 3; NGS, next generation sequencing; DAPI, 4',6'-diamidino-2-phenylindole.

Discussion

Although ART has progressed at a tremendous pace over the last 40 years, still up to 70% of the human embryos fail to complete preimplantation development and reach the blastocyst stage (Mertzanidou *et al.*, 2013a,b). Identification of causes of early embryo development failure requires a deeper understanding of the molecular mechanisms regulating preimplantation development and especially lineage differentiation. However, the current potential to explain failure in development is rather limited since most of our knowledge is acquired from research in model organisms. The need for human studies is further enhanced following the recent identification of major interspecies differences in the molecular pathways regulating first and second lineage segregation (Fogarty *et al.*, 2017; Gerri *et al.*, 2020; Stamatiadis *et al.*, 2021).

Novel technologies, such as CRISPR-Cas9, have revolutionized the field of developmental biology, offering the ability to functionally investigate the role of the genes by editing the genome directly in the developing human embryos in a simple and highly efficient manner. In this study, we aimed to investigate the role of Tead4/*TEAD4* in mouse and human preimplantation development, and more specifically TE differentiation, by targeting *Tead4*/*TEAD4* and creating knock-out embryos. The effects of targeting were examined by assessment of the developmental capacity and expression of lineage-specific markers representative of the TE and ICM lineage.

We first examined *Tead4* expression in media-control mouse embryos during preimplantation development. A clear difference in the pattern of *Tead4* expression between the ICM and TE lineage of blastocyst stage embryos was observed. Tead4 immunofluorescence signal was downregulated in the ICM compared with the TE lineage. This observation is consistent with previous findings on *Tead4* expression (Nothias *et al.*, 1995; Schultz, 2002; Yagi *et al.*, 2007; Nishioka *et al.*, 2008; Hirate *et al.*, 2012). We further identified positive *Tead4* expression in the nuclei of blastomeres from various developmental stages in mouse (four-, eight-cell, morula and blastocyst), suggesting that *Tead4* expression is initiated during EGA and remains constitutively nuclear. This finding differs from the previously proposed model by Home *et al.*, in which subcellular localization of Tead4 shifts between nucleus and cytoplasm during preimplantation development. This controlled subcellular localization of Tead4 was proposed to have a regulatory role in first lineage commitment. Home et al. (2012) described that in outer cells of the developing embryo, Tead4 is localized in the nucleus initiating the TE differentiation program, in contrast to the inner cells, which lack nuclear localization of Tead4 and differentiate towards the ICM. In contrast to the previous observations, we have identified that Tead4 remains constitutively localized in the nucleus. Our finding supports models proposing that gene expression differences between the ICM and TE lineages are the result of co-operative action between *Tead4* and the downstream components of the Hippo pathway (Nishioka *et al.*, 2009).

Introduction of gRNA1-Cas9-induced targeted genomic modification of the mouse *Tead4* locus and significantly compromised embryo development rates. Following 4 days of *in vitro* culture, 44.87% of the embryos arrested at the morula stage. Immunofluorescence analysis confirmed downregulation of Tead4 protein expression and also identified subsequent downregulation of the TE markers Cdx2 and Gata3 following *Tead4* targeting. These findings support the importance of *Tead4* acting upstream of the TE lineage specifiers *Cdx2* and *Gata3*, as it has been previously reported (Yagi *et al.*, 2007; Nishioka *et al.*, 2008). Loss of *Cdx2* expression led to the reported compromised embryo development rates as Cdx2 has been shown to be required for correct differentiation of the TE lineage and subsequent blastocoel formation (Strumpf *et al.*, 2005). A low percentage of the embryos (8.97%) were able to form high-quality Grade 3 blastocyst and retained expression of *Cdx2* in two to three cells in single confocal sections, while *Tead4* expression was successfully diminished in embryos carrying only frameshift mutations. This finding indicates the presence of alternative pathways inducing *Cdx2* expression, acting in parallel to *Tead4* towards TE differentiation. It has been previously shown that Notch and Hippo act in parallel and converge on *Cdx2* during the first lineage segregation in the blastocyst (Rayon *et al.*, 2014). Another involved mechanism is the autoregulation of *Cdx2*, which is sufficient to maintain and stabilize *Cdx2* expression levels (Niwa *et al.*, 2005; Cockburn and Rossant, 2010; Barros *et al.*, 2011).

Expression of pluripotency markers *Pou5f1* and *Sox2* was compared between mouse *Tead4*-targeted and media-control blastocyst stage embryos. *Sox2* is the gatekeeper of pluripotency and is the earliest marker expressed in the inner cells prior to ICM formation (Avilion *et al.*, 2003; Guo *et al.*, 2010). *Pou5f1* is necessary for the maintenance of pluripotency and is known to have a reciprocal relationship with the TE marker Cdx2 (Nichols *et al.*, 1998; Niwa *et al.*, 2005). Downregulation of Cdx2 due to *Tead4* targeting, suppressed TE lineage segregation and resulted in the outer cells ectopically expressing *Pou5f1*, confirming their reciprocal relationship. The $Sox2^{+}$ cell population remained unchanged between *Tead4*-targeted and media-control blastocysts. Taken together, our immunostaining data suggest that *Tead4* expression is required for successful differentiation and development of TE but is dispensable for the expression of ICM markers *Pou5f1* and *Sox2*.

Finally in mouse, application of the post-implantation model identified a proportion of *Tead4*-targeted plated embryos able to attach and progress towards the formation of egg-cylinder-like structures, in the absence of the characteristic trophoblast giant cells. Our observation on the ability of embryos to attach support the partial functional integrity of the TE following *Tead4*-targeting, which was also responsible for formation of the blastocoel cavity in blastocyst stage embryos, as it has been shown to require TE differentiation (Kidder and Watson, 2005). The formation of egg-cylinder-like structures further supports the dispensability of *Tead4* following implantation, which has been previously reported (Yagi *et al.*, 2007). However, the egg-cylinder-like structures were not analysed by NGS, which is a shortcoming of our study, as the resultant phenotype might be, in part, due to attachment of not completely edited or mosaic embryos, which retained functional Tead4 protein. Our post-implantation model results partially agree with the knock-out study by Kaneko and DePamphilis (2013), in which the authors showed that following A.T. treatment $Tead4^{-/-}$ produce outgrowths and form of trophoblast giant cells. The authors further proceeded and genotyped the outgrowths, confirming they were $Tead4^{-/-}$. However, in a more recent study, Israel *et al.* (2019) utilized the TRIM21-mediated protein depletion method to target Tead4 protein, and found that outgrowth formation was strongly impaired in Tead4-depleted embryos and that outgrowths were not formed.

In human, we aimed to investigate the pattern of *TEAD4* expression during the preimplantation stages and compare it to the mouse. *TEAD4* was found to be expressed following EGA and was identified in the cytoplasm of eight-cell embryos. Transition to the 16-cell stage was accompanied by TEAD4 translocation to the nucleus. The timing of translocation coincides with the initiation of bone morphogenetic protein 4 (*BMP4*) expression (Blakeley *et al.*, 2015). Studies in hESCs show that BMP4 treatment induces TEAD4 nuclear localization, suggesting that the same mechanism might be present in the human embryos and should be further investigated (Home *et al.*, 2012). Expression of the ICM marker *SOX2* was identified in 8-cell stage embryos, earlier than the 16-cell stage expression in mouse, pointing to distinct developmental programmes between species.

We further applied our CRISPR-Cas9 methodology to target *TEAD4* in the human germline aiming to examine the biological relevance of *TEAD4* in human TE differentiation. Recent data suggested the presence of an evolutionary conserved molecular cascade responsible for the initiation of the TE differentiation upstream of *TEAD4* between human, cow and mouse (Gerri *et al.*, 2020). In our study, we aimed to shed light on the mechanisms regulating TE differentiation downstream of *TEAD4*, with an emphasis on the transcription factors CDX2 and GATA3, which were previously shown to be downstream targets of *Tead4* in mouse, orchestrating TE lineage differentiation.

CRISPR-Cas9 was introduced in human MII oocytes along with sperm, which differs from the PN stage introduction in mouse. We have previously shown by targeting of *Pou5f1* in mouse that the timing of introduction does not affect subsequent experimental outcomes, as

editing efficiencies do not differ and editing is completed prior to the initiation of gene expression (Stamatiadis *et al.*, 2021). In this study, our previous statement is supported by the fact that a maximum of four different alleles were detected following CRISPR-Cas9 targeting, which corresponds to the DNA content of a two-cell embryo. The developmental capacity of targeted embryos was not affected, and embryo development rates did not differ significantly from the control group. NGS analysis and immunostaining confirmed successful targeting and the ability of complete knock-out embryos carrying exclusively frameshift *TEAD4* mutations to reach the blastocyst stage. However, while the developmental potential remained unaffected, blastocyst morphology was significantly compromised as all targeted generated blastocysts showed Grade C TE scores, with TE containing very few cells.

A CDX2 signal was not detected in CRISPR-Cas9-targeted human embryos, partially explaining the defects in the TE morphology. Expression of the ICM marker *SOX2* remained unaffected. Finally, we identified a major interspecies difference with mouse, since *GATA3* expression remained unaffected in *TEAD4*-targeted human embryos. This suggests that GATA3 does not function downstream of TEAD4 in human but acts in parallel to TEAD4/CDX2 towards TE differentiation, indicating distinct mechanisms of TE differentiation between mouse and human. Our data enhance the role of *GATA3*, as *GATA3* expression is enough to maintain TE differentiation in the absence of *CDX2* expression, and are in line with what has been previously described in hESCs. Targeted elimination of *TEAD4* during trophoblast transition in hESCs did not affect *GATA3* expression, similar to what we observed, indicating that the signalling pathways responsible for early TE lineage differentiation are divergent between mouse and human (Xiao *et al.*, 2020).

In our experiments, mouse and human embryos were cultured under the same conditions—low oxygen (5% O_2). The observed differences between the mouse and human might, in part, be due to the culture conditions and especially O_2 tension, which may variably affect *Tead4/TEAD4* targeted mouse and human embryos. The importance of *Tead4* in cell metabolism has been highlighted in mouse studies, where it was shown to promote mitochondrial transcription and to be essential for the establishment of oxidative energy metabolism, which is necessary for TE lineage development (Kumar *et al.*, 2018). Furthermore, Kaneko and DePamphilis (2013) discovered that by lowering O_2 concentration from 21% to 5%, a significantly higher percentage of *Tead4*-targeted mouse embryos were able to form a visible blastocoel cavity. However, Israel *et al.* (2019) observed no differences in the development rates of mouse embryos by lowering O_2 concentration following targeted degradation of Tead4 protein. Since the role of *TEAD4* in energy metabolism in human embryos has not been examined yet, and interspecies differences on the role of key lineage specifier genes have been previously identified, we cannot exclude the possibility that the observed differences between mouse and human are the result of variable effects triggered by the culture conditions, which were however similar for both mouse and human embryos in this study.

Overall, we perturbed the expression of *Tead4/TEAD4* with very high efficiency in mouse and human embryos. In mouse, we confirmed previous findings, with *Tead4* being a master regulator of TE differentiation upstream of *Cdx2* and *Gata3*. In human, we identified a distinct developmental programme, with *GATA3* acting in parallel with TEAD4/CDX2. In this context, it would be highly informative in the future to perform transcriptomic comparisons between *TEAD4*-targeted and media-control human embryos aiming to identify genes that are differentially expressed between the two populations (TEAD4−, GATA3+ vs TEAD4+, GATA3+), in an attempt to shed light on the molecular network regulating TE differentiation in human. Furthermore, identification of the mechanisms acting downstream will help us to elucidate if the pathways are distinct or branch downstream and co-activate the same set of genes.

Supplementary data

Supplementary data are available at *Human Reproduction* online.

Data availability

The data underlying this article are available in the article and its online Supplementary Material.

Authors' roles

P.S. conceived the project, designed the study, and performed the experiments in Figs.1 –4. P.S. and G.C. performed the experiments in Supplementary Fig. S1. P.S. and A.B. performed the data analysis. P.S. wrote the article. B.H., P.C., F.L., S.M.C.S.L., D.S., P.D.S., B.M., G.C. and A.B. contributed to the study design and interpreted the data. All authors reviewed the article and approved the final version.

Funding

The research was funded by the FWO-Vlaanderen (Flemish fund for scientific research, Grant no. G051516N), and Hercules funding (FWO.HMZ.2016.00.02.01) and Ghent University (BOF.BAS.2018.0018.01). Ferring Pharmaceuticals (Aalst, Belgium) provided an unrestricted educational grant. GC is supported by FWO-Vlaanderen (Flemish fund for scientific research, Grant no. 11L8822N). AB is supported by FWO-Vlaanderen (Flemish fund for scientific research, Grant no. 1298722N).

Conflict of interest

The authors declare no competing interests.

References

Auman HJ, Nottoli T, Lakiza O, Winger Q, Donaldson S, Williams T. Transcription factor AP-2γ is essential in the extra-embryonic lineages for early postimplantation development. *Development* 2002;**129**:2733–2747.

Avilion AA, Nicolis SK, Pevny LH, Perez L, Vivian N, Lovell-Badge R. Multipotent cell lineages in early mouse development depend on SOX2 function. *Genes Dev* 2003;**17**:126–140.

Barros R, Costa LD, Pinto-de-Sousa J, Duluc I, Freund JN, David L, Almeida R. CDX2 autoregulation in human intestinal metaplasia of

the stomach: impact on the stability of the phenotype. *Gut* 2011; **60**:290–298.

Bedzhov I, Leung CY, Bialecka M, Zernicka-Goetz M. In vitro culture of mouse blastocysts beyond the implantation stages. *Nat Protoc* 2014;**9**:2732–2739.

Bessonnard S, Mot LD, Gonze D, Barriol M, Dennis C, Goldbeter A, Dupont G, Chazaud C. Gata6, Nanog and Erk signaling control cell fate in the inner cell mass through a tristable regulatory network. *Development* 2014;**141**:3637–3648.

Blakeley P, Fogarty NME, del Valle I, Wamaitha SE, Hu TX, Elder K, Snell P, Christie L, Robson P, Niakan KK. Defining the three cell lineages of the human blastocyst by single-cell RNA-seq. *Development* 2015;**142**:3151–3165.

Boel A, Steyaert W, Rocker ND, Menten B, Callewaert B, Paepe AD, Coucke P, Willaert A. BATCH-GE: batch analysis of next-generation sequencing data for genome editing assessment. *Sci Rep* 2016;**6**:30330.

Chen L, Yabuuchi A, Eminli S, Takeuchi A, Lu CW, Hochedlinger K, Daley GQ. Cross-regulation of the Nanog and Cdx2 promoters. *Cell Res* 2009;**19**:1052–1061.

Cheng TC, Huang CC, Huang LS, Chen CI, Lee MS, Liu JY. Evaluation of mouse blastocyst implantation rate by morphology grading. *Chin J Physiol* 2004;**47**:43–47.

Choi I, Carey TS, Wilson CA, Knott JG. Transcription factor AP-2γ is a core regulator of tight junction biogenesis and cavity formation during mouse early embryogenesis. *Development* 2012;**139**: 4623–4632.

Cockburn K, Rossant J. Making the blastocyst: lessons from the mouse. *J Clin Invest* 2010;**120**:995–1003.

Fogarty NME, McCarthy A, Snijders KE, Powell BE, Kubikova N, Blakeley P, Lea R, Elder K, Wamaitha SE, Kim D *et al.* Genome editing reveals a role for OCT4 in human embryogenesis. *Nature* 2017;**550**:67–73.

Gerri C, McCarthy A, Alanis-Lobato G, Demtschenko A, Bruneau A, Loubersac S, Fogarty NME, Hampshire D, Elder K, Snell P *et al.* Initiation of a conserved trophectoderm program in human, cow and mouse embryos. *Nature* 2020;**587**:443–447.

Guo G, Huss M, Tong GQ, Wang C, Li Sun L, Clarke ND, Robson P. Resolution of cell fate decisions revealed by single-cell gene expression analysis from zygote to blastocyst. *Dev Cell* 2010;**18**: 675–685.

Heurtier V, Owens N, Gonzalez I, Mueller F, Proux C, Mornico D, Clerc P, Dubois A, Navarro P. The molecular logic of Nanog-induced self-renewal in mouse embryonic stem cells. *Nat Commun* 2019;**10**:

Hirate Y, Cockburn K, Rossant J, Sasaki H. Tead4 is constitutively nuclear, while nuclear vs. cytoplasmic Yap distribution is regulated in preimplantation mouse embryos. *Proc Natl Acad Sci U S A* 2012.

Home P, Ray S, Dutta D, Bronshteyn I, Larson M, Paul S. GATA3 is selectively expressed in the trophectoderm of peri-implantation embryo and directly regulates Cdx2 gene expression. *J Biol Chem* 2009.

Home P, Saha B, Ray S, Dutta D, Gunewardena S, Yoo B, Pal A, Vivian JL, Larson M, Petroff M *et al.* Altered subcellular localization of transcription factor TEAD4 regulates first mammalian cell lineage commitment. *Proc Natl Acad Sci U S A* 2012;**109**:7362–7367.

Israel S, Casser E, Drexler HCA, Fuellen G, Boiani M. A framework for TRIM21-mediated protein depletion in early mouse embryos: recapitulation of Tead4 null phenotype over three days. *BMC Genomics* 2019;**20**:1–19.

Kaneko KJ, DePamphilis ML. TEAD4 establishes the energy homeostasis essential for blastocoel formation. *Development* 2013;**140**: 3680–3690.

Keramari M, Razavi J, Ingman KA, Patsch C, Edenhofer F, Ward CM, Kimber SJ. Sox2 is essential for formation of trophectoderm in the preimplantation embryo. *PLoS One* 2010;**5**:e13952.

Kidder GM, Watson AJ. Roles of Na,K-ATPase in early development and trophectoderm differentiation. *Semin Nephrol* 2005;**25**:352–355.

Knott JG, Paul S. Transcriptional regulators of the trophoblast lineage in mammals with hemochorial placentation. *Reproduction* 2014; **148**:R121–R136.

Kumar RP, Ray S, Home P, Saha B, Bhattacharya B, Wilkins HM, Chavan H, Ganguly A, Milano-Foster J, Paul A *et al.* Regulation of energy metabolism during early mammalian development: Tead4 controls mitochondrial transcription. *Dev* 2018;**145**:https://doi.org/10.1242/dev.162644.

Labun K, Montague TG, Krause M, Torres Cleuren YN, Tjeldnes H, Valen E. CHOPCHOP v3: expanding the CRISPR web toolbox beyond genome editing. *Nucleic Acids Res* 2019.

Lorthongpanich C, Messerschmidt DM, Chan SW, Hong W, Knowles BB, Solter D. Temporal reduction of LATS kinases in the early preimplantation embryo prevents ICM lineage differentiation. *Genes Dev* 2013;**27**:1441–1446.

Mahoney WM, Hong JH, Yaffe MB, Farrance IKG. The transcriptional co-activator TAZ interacts differentially with transcriptional enhancer factor-1 (TEF-1) family members. *Biochem J* 2005.

Mertzanidou A, Spits C, Nguyen HT, Velde H, Van De Sermon K. Evolution of aneuploidy up to day 4 of human preimplantation development. *Hum Reprod* 2013a;**28**:1716–1724.

Mertzanidou A, Wilton L, Cheng J, Spits C, Vanneste E, Moreau Y, Vermeesch JR, Sermon K. Microarray analysis reveals abnormal chromosomal complements in over 70% of 14 normally developing human embryos. *Hum Reprod* 2013b;**28**:256–264.

Mihajlović AI, Bruce AW. The first cell-fate decision of mouse preimplantation embryo development: integrating cell position and polarity. *Open Biol* 2017;**7**:https://doi.org/10.1098/rsob.170210.

Miller A, Hendrich B. Chromatin remodelling proteins and cell fate decisions in mammalian preimplantation development. *Adv Anat Embryol Cell Biol* 2018.

Mitsui K, Tokuzawa Y, Itoh H, Segawa K, Murakami M, Takahashi K, Maruyama M, Maeda M, Yamanaka S. The homeoprotein nanog is required for maintenance of pluripotency in mouse epiblast and ES cells. *Cell* 2003;**113**:631–642.

Mulas C, Chia G, Jones KA, Hodgson AC, Stirparo GG, Nichols J. Oct4 regulates the embryonic axis and coordinates exit from pluripotency and germ layer specification in the mouse embryo. *Development* 2018.

Nichols J, Zevnik B, Anastassiadis K, Niwa H, Klewe-Nebenius D, Chambers I, Schöler H, Smith A. Formation of pluripotent stem cells in the mammalian embryo depends on the POU transcription factor Oct4. *Cell* 1998;**95**:379–391.

Nishioka N, Inoue K, ichi Adachi K, Kiyonari H, Ota M, Ralston A, Yabuta N, Hirahara S, Stephenson RO, Ogonuki N *et al.* The

Hippo signaling pathway components Lats and Yap pattern Tead4 activity to distinguish mouse trophectoderm from inner cell mass. *Dev Cell* 2009;**16**:398–410.

Nishioka N, Yamamoto S, Kiyonari H, Sato H, Sawada A, Ota M, Nakao K, Sasaki H. Tead4 is required for specification of trophectoderm in pre-implantation mouse embryos. *Mech Dev* 2008;**125**: 270–283.

Niwa H, Toyooka Y, Shimosato D, Strumpf D, Takahashi K, Yagi R, Rossant J. Interaction between Oct3/4 and Cdx2 determines trophectoderm differentiation. *Cell* 2005;**123**:917–929.

Nothias JY, Majumder S, Kaneko KJ, DePamphilis ML. Regulation of gene expression at the beginning of mammalian development. *J Biol Chem* 1995.

Palmieri SL, Peter W, Hess H, Schöler HR. Oct-4 transcription factor is differentially expressed in the mouse embryo during establishment of the first two extraembryonic cell lineages involved in implantation. *Dev Biol* 1994.

Paul S, Knott JG. Epigenetic control of cell fate in mouse blastocysts: The role of covalent histone modifications and chromatin remodeling. *Mol Reprod Dev* 2014.

Ralston A, Cox BJ, Nishioka N, Sasaki H, Chea E, Rugg-Gunn P, Guo G, Robson P, Draper JS, Rossant J. Gata3 regulates trophoblast development downstream of Tead4 and in parallel to Cdx2. *Development* 2010;**137**:395–403.

Rayon T, Menchero S, Nieto A, Xenopoulos P, Crespo M, Cockburn K, Cañon S, Sasaki H, Hadjantonakis AK, la Pompa JL et al Notch and hippo converge on Cdx2 to specify the trophectoderm lineage in the mouse blastocyst. *Dev Cell* 2014;**30**:410–422.

Schoolcraft WB, Gardner DK, Lane M, Schlenker T, Hamilton F, Meldrum DR. Blastocyst culture and transfer: analysis of results and parameters affecting outcome in two in vitro fertilization programs. *Fertil Steril* 1999;**72**:604–609.

Schultz RM. The molecular foundations of the maternal to zygotic transition in the preimplantation embryo. *Hum Reprod Update* 2002.

Stamatiadis P, Boel A, Cosemans G, Popovic M, Bekaert B, Guggilla R, Tang M, Sutter P, De Nieuwerburgh F, Van Menten B *et al*. Comparative analysis of mouse and human preimplantation development following POU5F1 CRISPR/Cas9 targeting reveals interspecies differences. *Hum Reprod* 2021;**36**:1242–1252.

Stephenson RO, Rossant J, Tam PPL. Intercellular interactions, position, and polarity in establishing blastocyst cell lineages and embryonic axes. *Cold Spring Harb Perspect Biol* 2012;**4**:a008235.

Strumpf D, Mao CA, Yamanaka Y, Ralston A, Chawengsaksophak K, Beck F, Rossant J. Cdx2 is required for correct cell fate specification and differentiation of trophectoderm in the mouse blastocyst. *Development* 2005;**132**:2093–2102.

Thomson M, Liu SJ, Zou LN, Smith Z, Meissner A, Ramanathan S. Pluripotency factors in embryonic stem cells regulate differentiation into germ layers. *Cell* 2011;**145**:875–889.

Tolkunova E, Cavaleri F, Eckardt S, Reinbold R, Christenson LK, Schöler HR, Tomilin A. The caudal -related protein Cdx2 promotes trophoblast differentiation of mouse embryonic stem cells. *Stem Cells* 2006;**24**:139–144.

Vassilev A, Kaneko KJ, Shu H, Zhao Y, DePamphilis ML. TEAD/TEF transcription factors utilize the activation domain of YAP65, a Src/Yes-associated protein localized in the cytoplasm. *Genes Dev* 2001.

Werling U, Schorle H. Transcription factor gene AP-2γ essential for early murine development. *Mol Cell Biol* 2002;**22**:3149–3156.

Winger Q, Huang J, Auman HJ, Lewandoski M, Williams T. Analysis of transcription factor AP-2 expression and function during mouse preimplantation development. *Biol Reprod* 2006;**75**: 324–333.

Xiao L, Ma L, Wang Z, Yu Y, Lye SJ, Shan Y, Wei Y. Deciphering a distinct regulatory network of TEAD4, CDX2 and GATA3 in humans for trophoblast transition from embryonic stem cells. *Biochim Biophys Acta Mol Cell Res* 2020;**1867**:118736.

Yagi R, Kohn MJ, Karavanova I, Kaneko KJ, Vullhorst D, DePamphilis ML, Buonanno A. Transcription factor TEAD4 specifies the trophectoderm lineage at the beginning of mammalian development. *Development* 2007;**134**:3827–3836.

Zhu M, Cornwall-Scoones J, Wang P, Handford CE, Na J, Thomson M, Zernicka-Goetz M. Developmental clock and mechanism of de novo polarization of the mouse embryo. *Science* 2020;**370**:https://doi.org/10.1126/science.abd270.

Zhu M, Leung CY, Shahbazi MN, Zernicka-Goetz M. Actomyosin polarisation through PLC-PKC triggers symmetry breaking of the mouse embryo. *Nat Commun* 2017;**8**:1–16.